



## **Error and precision of photogrammetry in the deep-sea**

**Samantha Peart, North Carolina State University, Raleigh, NC**

*Mentors: Katherine Dunlop and Brian Schlining*

*Summer 2015*

**Keywords: deep-sea ecology, correction factor, oblique photogrammetry, Remotely Operated Vehicle, climate change**

### **ABSTRACT**

The effects of climate change are well studied in oceanic surface waters and coastal areas, however, impacts are least known for the deep-sea. The Station M time series data set has been collected for 26 years to examine the effect of climate change on the deep-sea carbon cycle. As part of the time series, measurements of animal body size are gathered to calculate biomass and respiration rates. This is important to better define the role of deep-seafloor animals in the deep-sea carbon cycle. Measurements of deep-sea animals at Station M are made from Remotely Operated Vehicle (ROV) video footage using paired lasers and laser measurement algorithms. In this study ROV video data of a calibration target were collected at 4000 m and analyzed to quantify the effect of length and angle on measurement error. This data was used to develop a correction factor that can be used to achieve more accurate measurements of epibenthic megafauna.

### **1. INTRODUCTION**

Increasing water temperature, density stratification, and ocean acidification are well known effects of climate change in the world's oceans, yet the impacts of climate change are least known for the deep ocean (Smith et al., 2013; Ruhl et al., 2008). There is no consensus on the effects of climate change on the deep ocean. Increased stratification in the open ocean is thought to restrict the exchange of nutrients from deeper water to surface primary producers reducing the export of particulate organic carbon (POC) (food supply) to the deep ocean (Sherman and Smith, 2009; Ruhl et al., 2008). However, enhanced food supply to the abyssal northeast Pacific (~4000 m depth) has been observed in recent years, yet it is still unclear whether there might be an increasing trend in food supply at other deep ocean time-series stations (Smith et al., 2013). The amount of organic carbon that reaches the deep ocean and its ultimate utilization or long-term sequestration in the sediments is a major unknown component of the global carbon cycle (Smith et al., 2013). These knowledge gaps need to be filled as the deep ocean benthos is a key component of the carbon cycle and can affect long-term bioturbation, remineralization, and sequestration rates of carbon in the deep ocean (Ruhl et al., 2007).

Epibenthic megafauna (organisms  $\geq 1$  cm that occupy the surface layer of the seabed sediment and are visible in photographs) play a role in carbon sequestration (Dunlop et al., 2015). Epibenthic megafauna remineralise POC that sinks to the seafloor through respiration and regeneration (Ruhl et al., 2014). Faunal density and body size estimates were gathered using photogrammetric techniques and have been used to assess the respiratory demands of echinoderm assemblages from deep ocean habitats (Ruhl et al., 2014). Accurate and precise body size measurements to generate accurate biomass estimates will provide a better definition of the animal's role in the carbon cycle and make a significant contribution to the Station M time-series (Dunlop et al., 2015).

Measurements of deep ocean processes, atmospheric and surface ocean conditions have been collected as part of an ongoing 26-year time series at Station M (~4000 m water depth) at the Monterey Deep-sea Fan (Fig. 1)(Dunlop et al., 2015; Kuhnz et al., 2014; Smith et al., 2013). This data has substantially improved understanding of the connections between surface food supply and deep ocean benthic communities, as well as, the role of the deep ocean benthic environment in the global carbon cycle (Dunlop et al., 2015). Since 2006, Monterey Bay Aquarium Research Institute (MBARI) has measured megafauna body size at Station M from video recordings taken by a camera mounted on remotely operated vehicles (ROV) (Kuhnz et al., 2014; Dunlop et al., 2015). Scientists at MBARI have been able to measure megafauna in these recordings using the ROV's two parallel mounted lasers, spaced 29 cm apart, that serve as a scale bar. To achieve the most accurate measurements, the object must be placed precisely in a perpendicular orientation to the camera; if not, the associated difference needs to be corrected (Dunlop et al., 2015).

To store and manage MBARI's video footage software engineers have developed the MBARI Video Annotation and Reference System (VARS). This allowed researchers to create, store, and retrieve video annotations based on the ROV dive footage (Schlining and Stout, 2006). VARS has a "Distance Tool" that allows the user to calculate the distance between two points, which is used to measure the length of animals and objects in still frame grabs collected from video footage. Length is calculated by the user selecting two endpoints, VARS returning the x and y coordinates of these points, and then using VARS Query and a Python code to extract the x-coordinate distance, y-coordinate distance, and total distance (in pixels). The total distance in pixels is converted to cm using the known distance of the lasers aligned with the organism in the photo and the lasers' distance in pixels. However, all measurements must be taken on the same orientation as the laser line according to the Canadian Grid (Fig. 2). The grid shows that oblique photographs are more difficult to interpret quantitatively because spatial scales on a perspective image consistently change with distance from the bottom of the photograph (Wakefield and Genin, 1986). Therefore, the pixels at the top of an image are smaller and further apart than those at the bottom of the image, thus to achieve an accurate measurement the organism and the laser line must be in the same orientation.

This study aimed to use video data collected at Station M using the ROV Doc Ricketts, to (1) calculate the error and precision of measuring organisms at different lengths and angles on VARS and to (2) develop a correction factor that can be incorporated into the VARS Distance Tool algorithm to reduce errors associated with object orientation and the Canadian Grid. This study will allow more accurate measurements of epibenthic megafauna and biomass to be achieved, improving understandings of the role of epibenthic megafauna in the deep ocean carbon cycle.

## **2. METHODS**

A calibration board (48.5 x 48.5 cm) was placed on the seabed (4th April 2014) by the ROV Doc Ricketts at 4000 m at Station M. The ROV was flown over the board and video footage was recorded, from which still frame grabs were taken in VARS. Video footage and frame grabs of the board were recorded in the same manner as data would be collected on epibenthic megafauna during an ROV transect (ensuring that the paired lasers passed over the board).

### *2.1 Calculating error and precision*

Using the VARS distance tool, length measurements were taken across the distance between the lasers and twenty-four different length measurements 180° around the calibration board (n = 30). Angles in the first and fourth quadrants of the board were measured because the remaining two quadrants were mirror images. In order to replicate VARS measurements on the physical board a feature was measured that could be identified on the computer and in person. Therefore, measurements were taken from the center to the top far corner of squares on the calibration board (Fig. 3). The lengths of these measurements were calculated in the Distance Tool by multiplying the length's distance in pixels by the length between the lasers in centimeters (29 cm) and then dividing the result by the distance between the lasers in pixels.

The same measurements were made on the physical color calibration board (at sea level). Length measurements were taken by an engineering ruler and a protractor to determine the angle of each length from the laser lines. Lengths measured on the actual color calibration board were considered the “actual measurements.”

Error was calculated by taking the difference of the actual measurement and the VARS measurement. A Kruskal-Wallis statistical analysis was used to examine (1) the effect of measurement angle and (2) total length on measurement error and precision.

### *2.2 Recalculating error, eliminating angle as a factor*

To focus on the relationship between length and error, we reduced the effect of angle as a factor by measuring lengths a second time at angles 270°, 315°, 0°, 45°, and 90° (see Figure 4). At each respective angle, measurements were taken using the VARS Distance Tool at lengths: a third of the originally measured length (small), two-thirds of the original length (medium), and the full original length (large), thirty times each. These measurements were again measured on the physical calibration board, allowing us to calculate measurement error. A two-way ANOVA was used to examine the effect of length on measurement error.

### *2.3 Algorithm*

On Excel, equations that describe the relationships between angle and error, length and error were created to be incorporated into the correction factor.

Originally the VARS Distance Tool coding was written in Scala and had generic camera parameters. While translating this code into Matlab (R2015a 8.5.0.197613), we created a code that incorporates the height of the camera off the ground, height of the image in radians, width of the image in radians, and tilt of the camera in radians to determine the image width and height on the view plane. We then created a second code that incorporates the camera parameters, image

width and height in pixels, and the x and y coordinates of the pixels on the image to determine the x and y distance of the pixel on the image from the camera.

To evaluate the code results, the distance between the lasers was measured using the code. In VARS, one laser midpoint was selected as an endpoint and the other laser midpoint was selected as the other endpoint. Those endpoints were used as the X and Y coordinates of the pixels on the image in the second part of the code.

### **3. RESULTS**

#### *3.1 Error and precision analysis*

A Shapiro-Wilk normality test was ran which had a p-value  $< 2.2e^{-16}$  and the data also did not meet the ANOVA assumption of normality and homogeneity of variance (Fig. 5) (Bartlett test;  $p < 2.2e^{-16}$ ). Therefore a nonparametric Kruskal-Wallis rank sum test was used. This showed ...no significance? ( $p < 2.2e^{-16}$ ). Angle had a significant effect on measurement error ( $p = 3.27e^{-9}$ ), as does length ( $p = 0.000133$ ). However, we also found that length and angle have a significant interaction.

#### *3.2 Recalculating error, eliminating angle as a factor*

A Shapiro-Wilk normality test was ran and with a p-value  $< .05$  the data seemed to meet the assumptions of the ANOVA ( $p = 2.805e^{-5}$ ). Both angle ( $p < 2e^{-16}$ ) and length ( $p < 2e^{-16}$ ) had a significant effect on measurement error. However, the relationship between length and error were no longer significant ( $p = 0.236$ ).

#### *3.3 Algorithm*

A code was created in Matlab that successfully results in X and Y distances of pixels away from the bottom of the camera. To test the code, we measured the distance between the laser, which resulted in 10.34 cm, a little more than a third of the actual length of the lasers.

### **4. DISCUSSION**

Estimating biomass of epibenthic megafauna, using length measurement data, will help define their role in the deep-sea carbon cycle. Biomass is also required to calculate organic carbon utilization of epibenthic megafauna using wet-weight specific oxygen consumption rates of individual species (Dunlop et al., 2015; Ruhl et al., 2014). This will lead to a better understanding of the response of deep-sea benthic communities to climate related changes in food supply and their impact on biogeochemical cycling (Dunlop et al., 2015; Lauerman et al., 1996). Scientists have been using the ROV's paired lasers as a scale bar in measuring the size of animals recorded during video transects and they have found between 0.5 mm to -3.06 mm of mean error, depending on the orientation of the animal in relation to the lasers (Dunlop et al., 2015).

#### *4.1 Calculating error and precision*

Graphing and analyzing the effect of angle on the ROV length measurement mean error showed that more error was associated with measurements closer to a vertical orientation (positively towards 90° or negatively towards 270°) (Fig. 6). It was unexpected that vertical lengths had more error than diagonal lengths because Kuhnz et al. (2014) found vertical lengths to have a mean error of .46 mm (1.15%) as oppose to -3.06 mm (-5.38%) mean error found associated with diagonal lengths. Since the image perspective constantly changes with distance to the bottom of the photo (Wakefield and Genin, 1986), the disparity in distance from the bottom to the top of the image is creating more error than measurements diagonally across.

Figure 8 shows that angle has an effect on length, which would be expected because the closer you are to 45° the length is much longer than compared to 90° or 270°. It is likely that length appears to have as significant effect on error because of the strong pattern length and angle have on each other.

#### *4.2 Recalculating error, eliminating angle as a factor*

Exploring the relationship between length and error a second time, we reduced the effect of angle by measuring small, medium, and large lengths for five respective angles (see Figure 4). By doing so, the significant relationship between length and error became more evident. As length became longer there was more error was associated and precision decreased (see Figure 8).

#### *4.3 Algorithm*

The algorithm

## **5. CONCLUSIONS/RECOMMENDATIONS**

### **ACKNOWLEDGEMENTS**

I would like to thank Kathy Dunlop and Brian Schlining giving me an opportunity to work with them this summer and for mentoring me along the way. I would also like to thank Ken Smith and the Pelagic-Benthic Coupling Lab for mentoring me and offering assistance when I needed it this summer. George Matsumoto and Linda Kuhnz thank you for coordinating an amazing internship experience, you both went above and beyond providing me and the other interns with anything we could ever need or want. Also, Linda thank you for teaching me about VARS and photogrammetric techniques used within it. Marko and Ben thank you for helping Kathy and I take measurements and framegrabs on the Doc Ricketts. I would also like to thank my home institution, North Carolina State University, for making student license of Matlab available and the Office of Undergraduate Research for funding my travel to and from California for the summer

## REFERENCES

- Dunlop, K.M.,** L. Kuhnz, H. Ruhl, C. Huffard, D. Caress, R. Henthorn, B. Hobson, P. McGill, K. Smith (2015). An evaluation of deep-sea benthic megafauna length measurements obtained with laser and stereo camera methods. *Deep Sea Research Part I: Oceanographic Research Papers*, 96: 38-48. doi: 10.1016/j.dsr.2014.11.003
- Kuhnz, L.A.,** H. Ruhl, C. Huffard, K. Smith (2014). Rapid changes and long-term cycles in the benthic megafaunal community observed over 24 years in the abyssal northeast Pacific. *Progress in Oceanography*, 124: 1-11. doi:10.1016/j.pocean.2014.04.007.
- Lauerman, L.M.L.,** R. Kaufmann, K. Smith (1996). Distribution and abundance of epibenthic megafauna at a long time-series station in the abyssal northeast Pacific. *Deep Sea Research*. 43, 1075-1103. doi:10.1016/0967-0637(96) 00045-3.
- Ruhl, H.A.** (2007). Abundance and size distribution dynamics of abyssal epibenthic megafauna in the northeast Pacific. *Ecology*, 88: 1250-1262. doi:[10.1890/06-0890](https://doi.org/10.1890/06-0890)
- Ruhl, H.A.,** J. Ellena, K. Smith (2008). Connections between climate, food limitation, and carbon cycling in abyssal sediment communities. *Proceedings of the National Academy of Sciences*, 105: 17006-17011. doi: 10.1073/pnas.0803898105
- Ruhl, H.A.,** B. Brett, S. Hughes, C. Alt, E. Ross, R. Lampitt, C. Pebody, K. Smith, and D. Billett (2014). Links between deep-sea respiration and community dynamics. *Ecology*, 95: 1651-1662, doi:[10.1890/13-0675.1](https://doi.org/10.1890/13-0675.1)
- Schlining, B.** and N. Stout (2006). MBARI's Video Annotation and Reference System. *OCEANS*: 1-5. doi: [10.1109/OCEANS.2006.306879](https://doi.org/10.1109/OCEANS.2006.306879)
- Sherman, A.D., K.L. Smith, Jr.** (2009) Deep-sea benthic boundary layer communities and food supply: A long-term monitoring strategy. *Deep-Sea Res. II*, 56, 1754-1762. doi: [10.1016/0198-0149\(87\)90148-8](https://doi.org/10.1016/0198-0149(87)90148-8)
- Smith, K.L.,** H. Ruhl, M. Kahru, C. Huffard, A. Sherman (2013). Deep ocean communities impacted by changing climate over 24 y in the abyssal northeast Pacific Ocean. *Proceedings of the National Academy of Sciences*, 110: 19838-19841, doi: 10.1073/pnas.1315447110
- Wakefield, W.,** A. Genin (1986). The use of a Canadian (perspective) grid in deep-sea photography. *Deep Sea Research Part A. Oceanographic Research Papers*, 34: 469-478. doi:[10.1016/0198-0149\(87\)90148-8](https://doi.org/10.1016/0198-0149(87)90148-8)

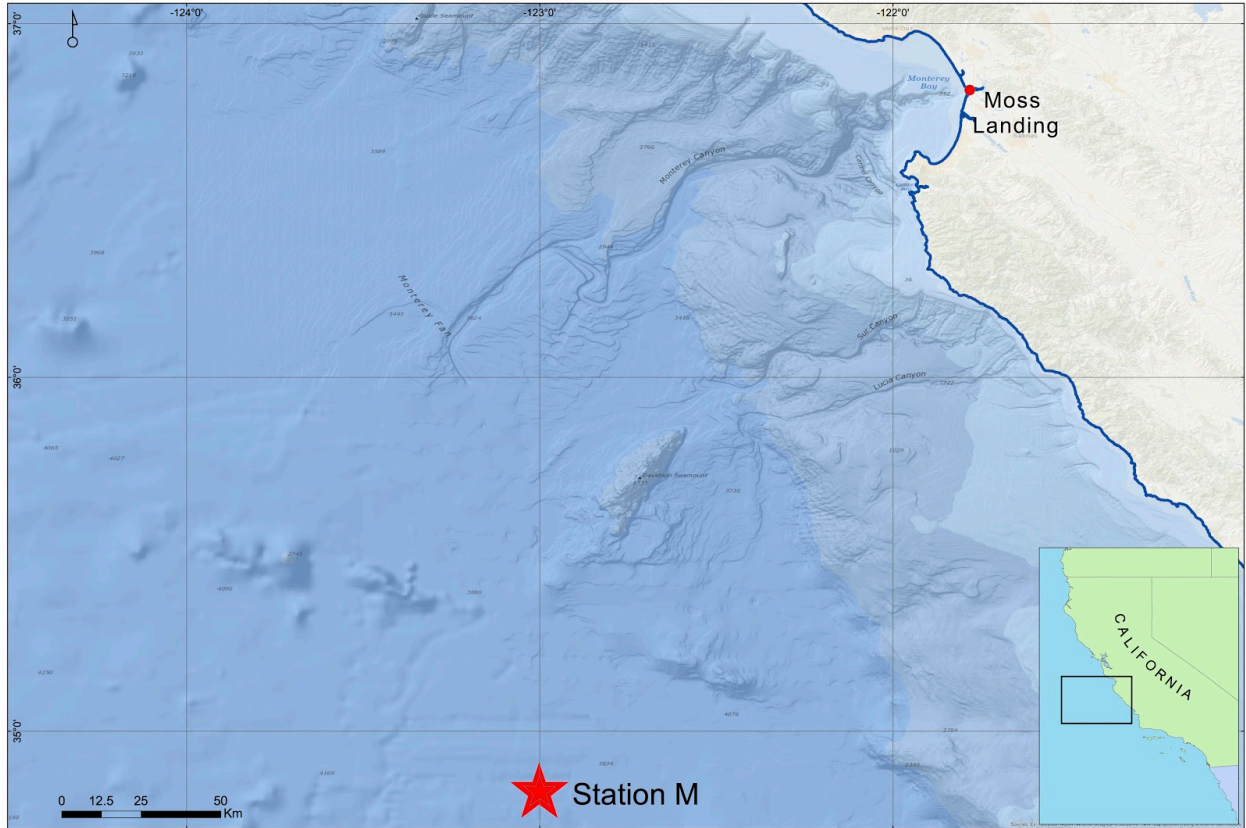


**Figure 1.** Map of the location of Station M in relation to the central coast of California.

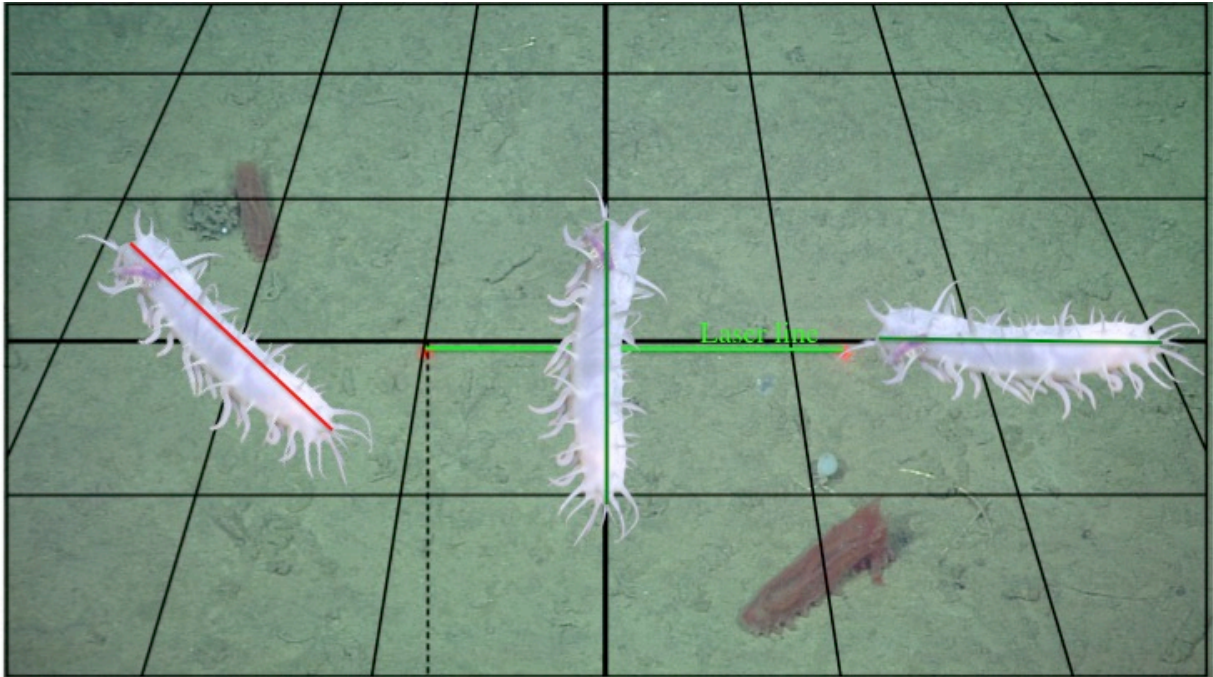


**Figure 2.** Diagram of a Video Annotation Reference System frame grab taken from video footage of the seafloor at Station M (~ 4000 m) superimposed with the Canadian Grid. The diagram illustrates individual holothurians, *Oneirophanta mutabilis*, aligned with the paired lasers in a) diagonal, b) vertical and c) horizontal orientations.

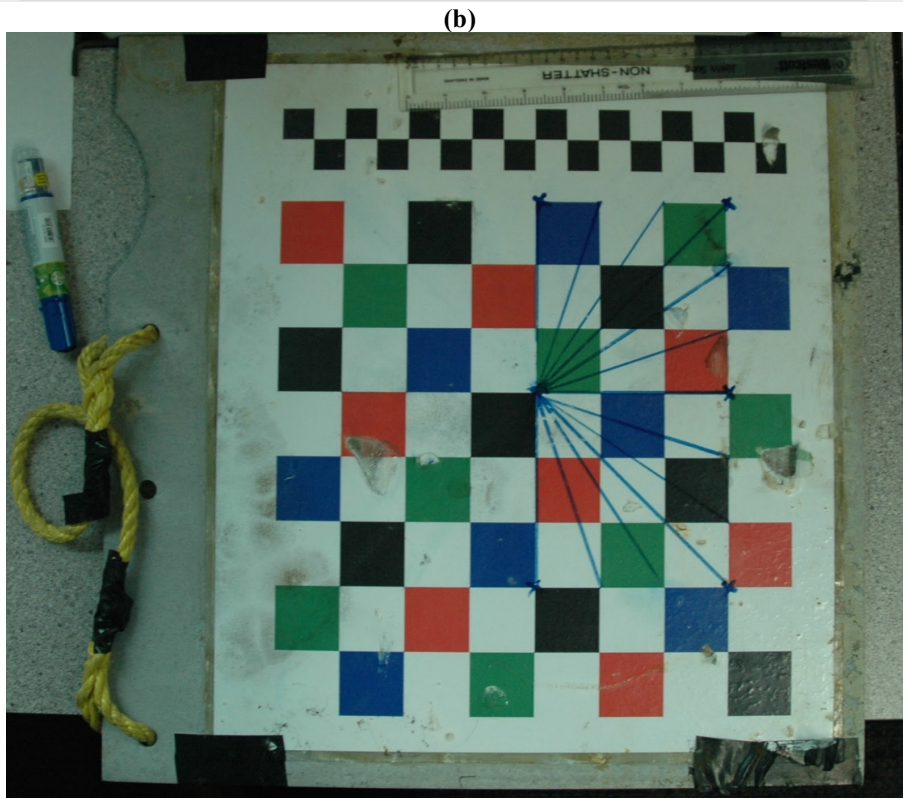


**Figure 3.** Diagram of the calibration board and measurement dimensions made at (a) ~4000 m at Station M and (b) at sea level.

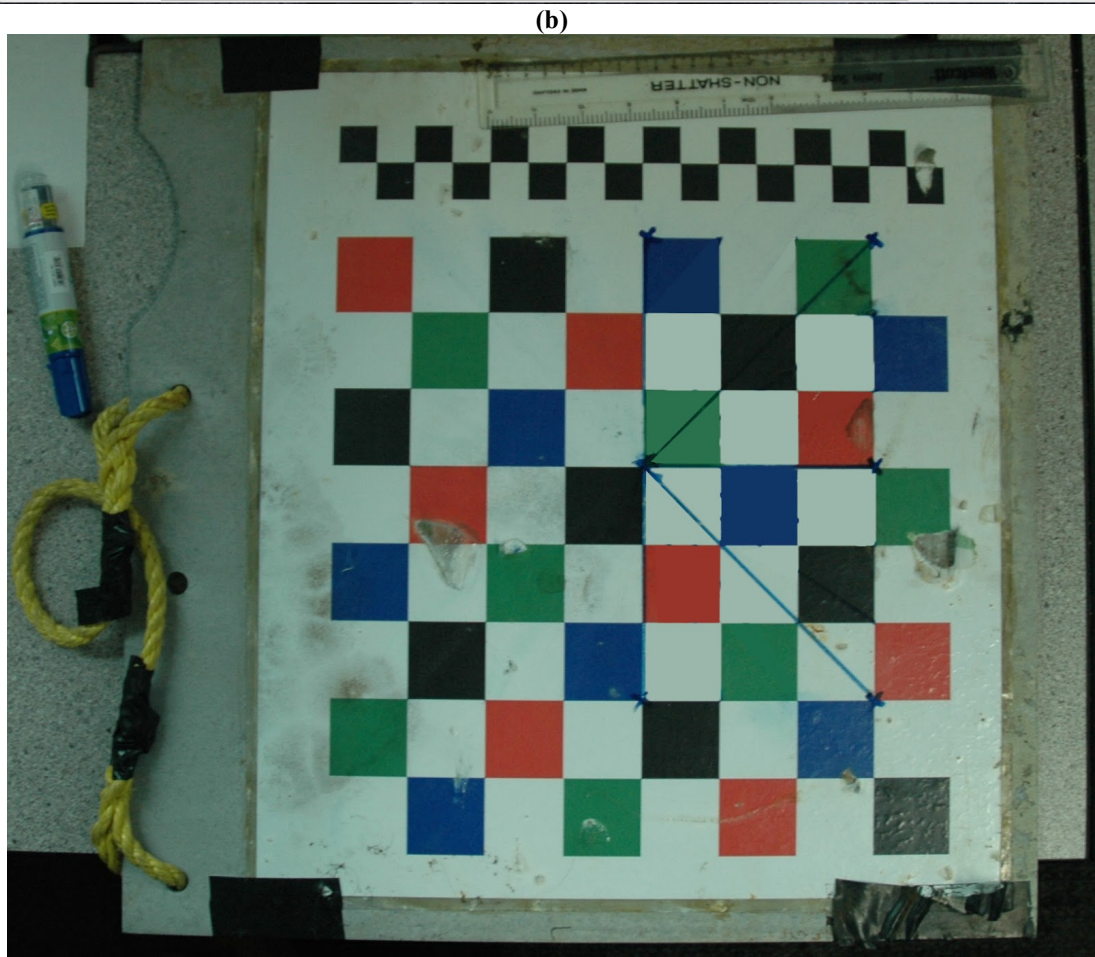
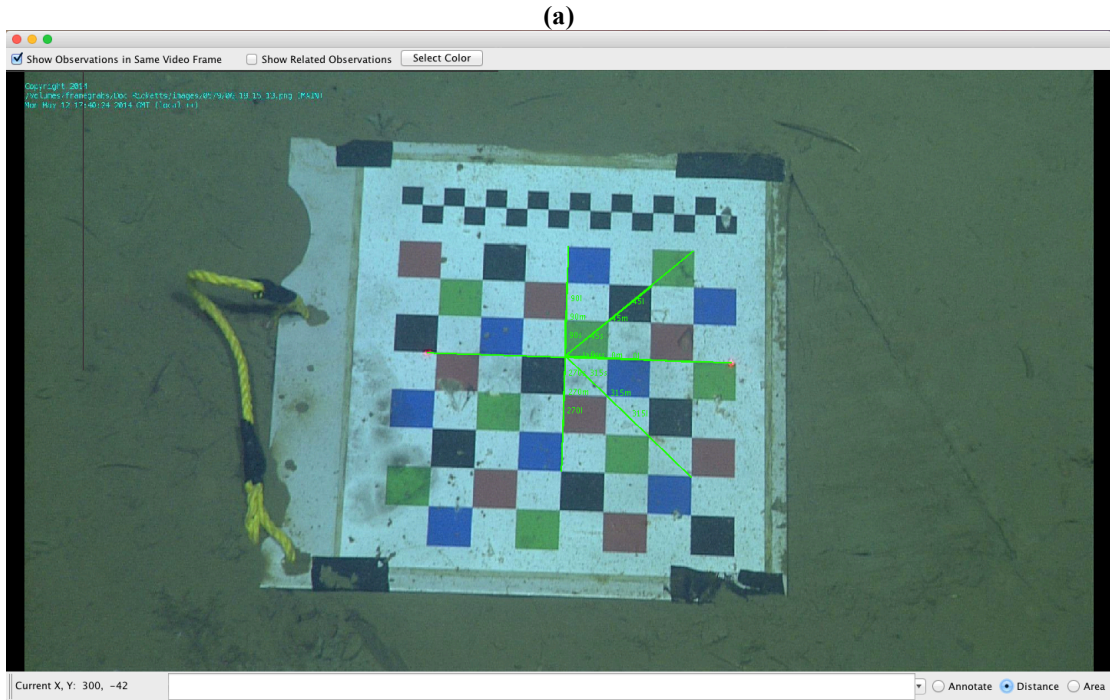


**Figure 4.** Annotated image of the calibration board and small, medium and large length measurements made at the angles 270°, 315°, 0°, 45°, and 90° at a) ~ 4000 m depth and b) sea level

**Figure 5.** The Shapiro-Wilk normality test showed the data did not meet the ANOVA assumptions of normality.

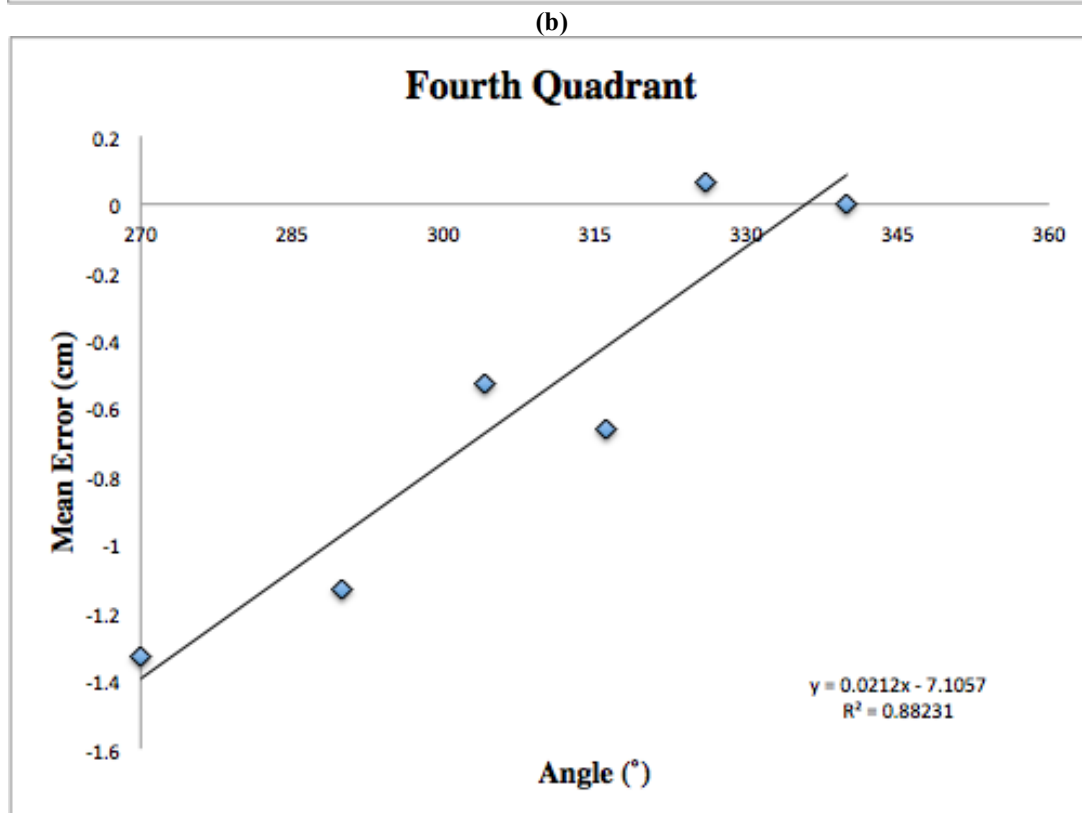
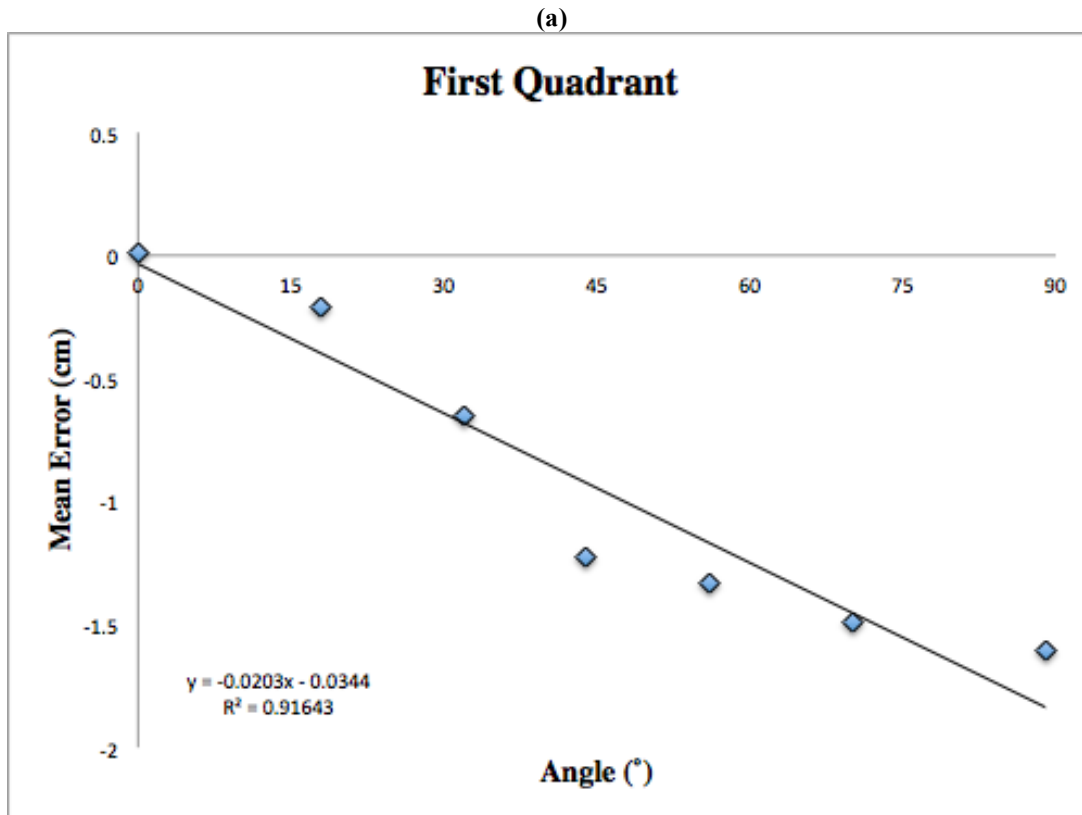
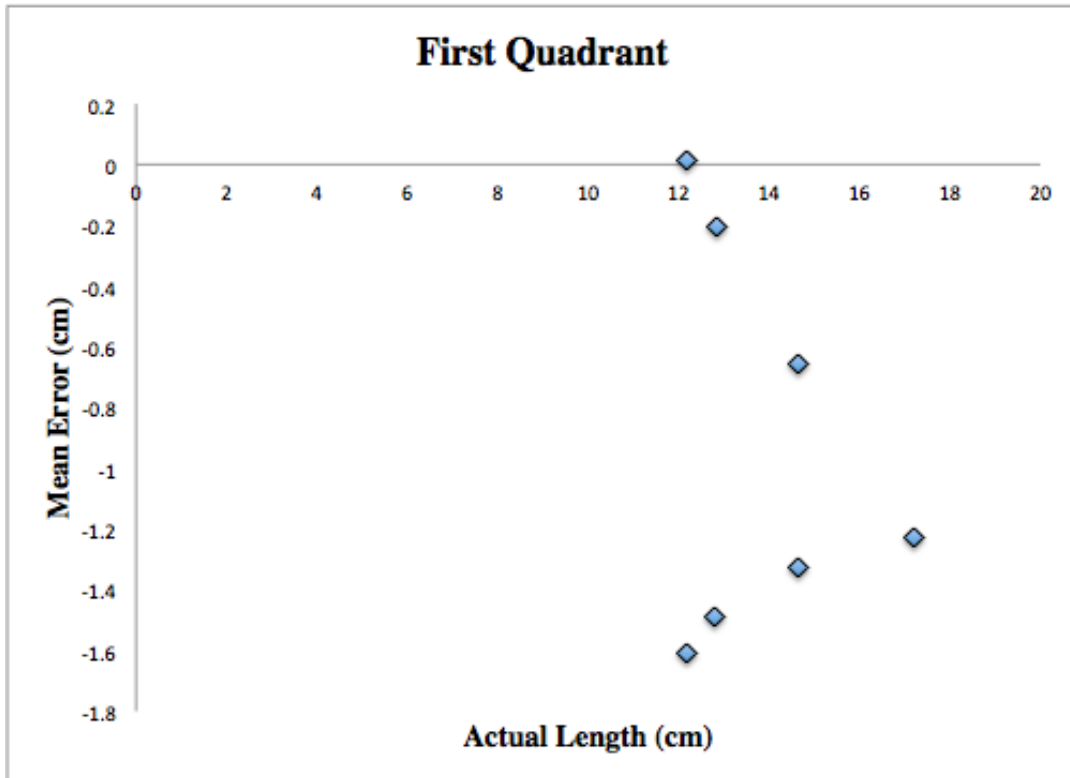


**Figure 6.** Scatterplots of the measurement angle plotted against the mean error ( $n=30$ ) made in the the a) first and b) second quadrants of the color calibration board.

(a)



(b)

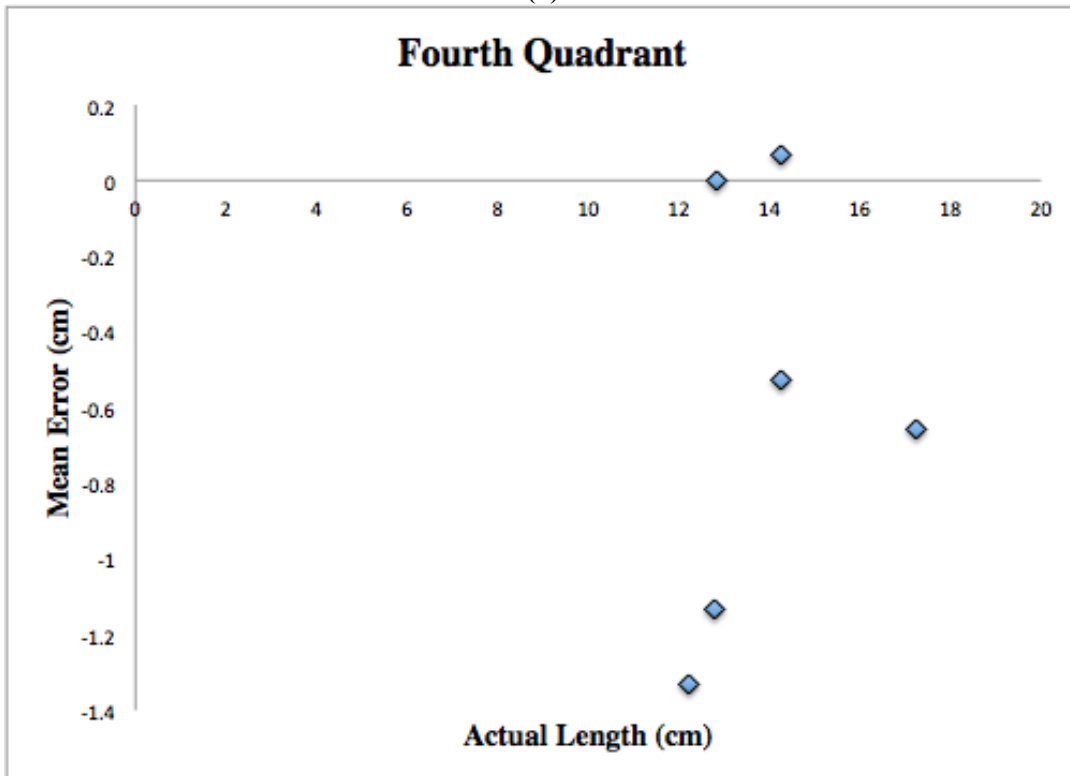
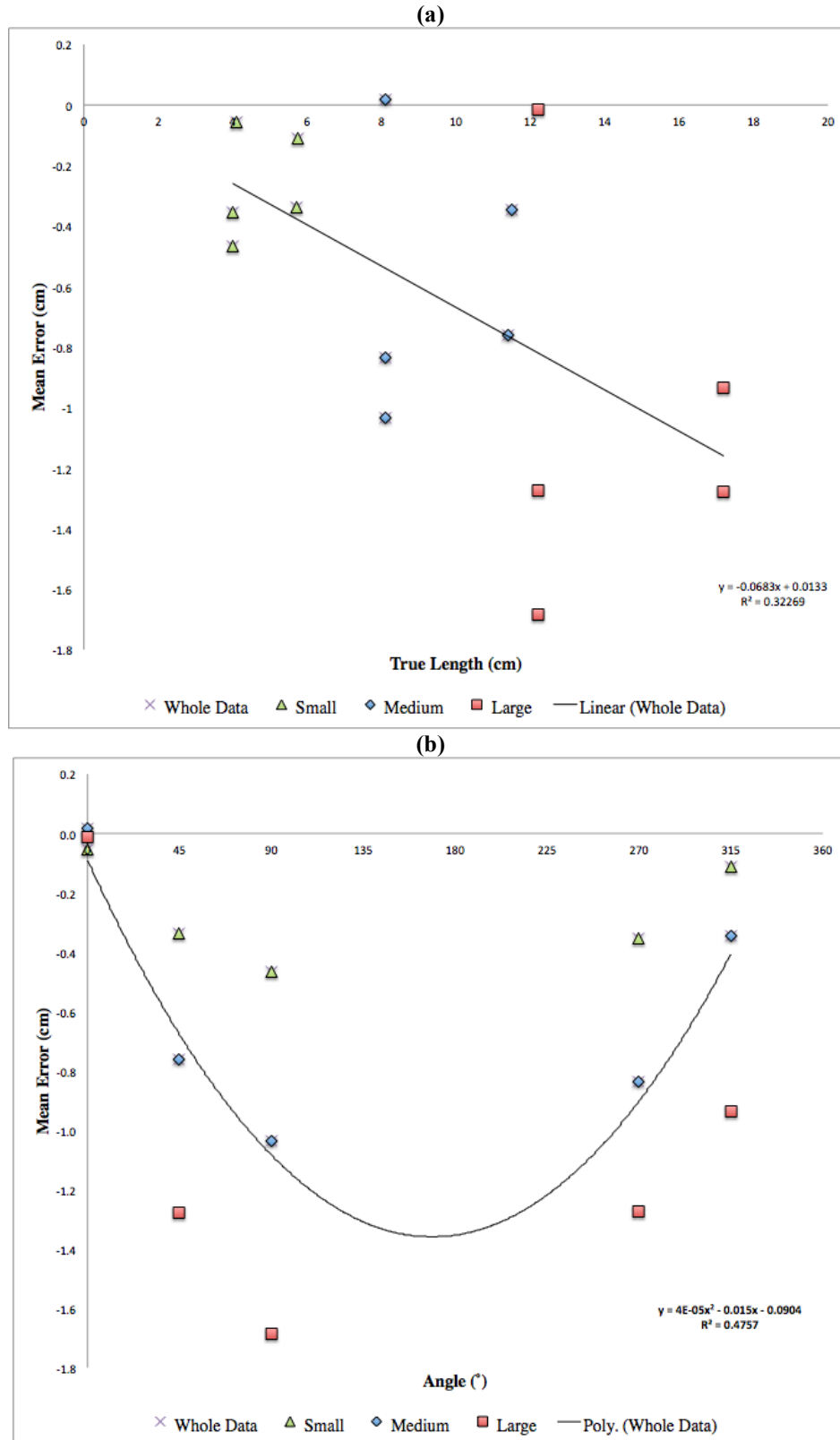


Figure 7. Scatterplot of actual length measurements, taken with a ruler on the physical calibration board, and mean error (n=30) on the a) first and b) fourth quadrants.



**Figure 8.** Scatterplots and trend lines of the (a) distribution of lengths with their associated errors; (b) lengths taken at different angles with their associated errors. “Small” lengths were taken a third of the way across the board, “medium” two-thirds, and “large” the full length.